21st SYMPOSIUM OF THE INDUSTRIAL APPLICATION OF GAS TURBINES COMMITTEE
BANFF, ALBERTA, CANADA
OCTOBER 19-21, 2015

2015-IAGT-201

Comparison of Gas Turbine Degradations Employed at Five Natural Gas Compressor Station Sites

K.K. Botros, C. Hartloper
NOVA Chemicals, Centre for Applied Research

and

H. Golshan, D. Rogers
TransCanada PipeLines Limited

Calgary, Alberta, Canada

Key Words: Gas Turbine Degradation, Engine Soak Wash, Gas Pipeline, Compressor Station, Turbine Performance.

Abstract

Gas Turbines employed in natural gas compressor stations are subject to recoverable and under-recoverable degradation mostly manifested in the decrease in the isentropic efficiency of the air compressor part of the engines. To counteract these decreases in compressor efficiency, it is standard procedure to 'wash' the engine from time to time. In compressor stations on gas transmission systems, engine washes are performed off-line and are scheduled in such intervals to optimize the maintenance procedure. This optimization requires accurate prediction of the performance degradation of the engine over time. A methodology is developed to evaluate the gas turbine degradation of all parts of the engine, and particularly the air compressor since it is most prone to fouling and degradation. This methodology combines Gas Path Analysis (GPA) to evaluate the thermodynamic parameters over the engine cycle followed by parameter estimation based on the Bayesian Error-in-Variable Model (EVM) to filter the data of possible noise due to measurement errors. The methodology quantifies the engine-performance degradation over time, and indicates the effectiveness of each engine wash. In the present paper, the methodology is applied to assess both recoverable and un-recoverable degradations of five gas turbine engines employed on TransCanada's pipeline system in Canada. These engines are: three GE LM2500+, one RR RB211-24G, and one GE LM1600 gas turbines. Hourly data were collected over the past 5-7 years, and engine health parameters were extracted to delineate the respective engine degradation and recovery post respective offline washes. The impacts of engine loading, site air quality conditions and site elevation on engine-air-compressor isentropic efficiency are compared between the five engines.

1. Introduction

Degradation in gas turbines (GT) is of great importance to industrial users for engine performance reliability and operating costs. Degradation refers to a drop in the performance of the GT engine indicated by a loss of available power and increased heat rate (or reduced thermal efficiency). In essence, degradation of the overall engine is a combined effect of the degradation contribution from each of its components, although each component of the engine degrades at a different rate [1]. Significant development has been made in determining the mechanisms of engine degradation [1-3]. Fouling, corrosion, and impingement of foreign objects on both the compressor and turbine blades are some of the mechanisms that cause engine degradation [1]. These factors contribute towards reduced tip clearance, change in blade geometry and surface roughness [2,3], which are manifested in a reduction in shaft power output and increase in the overall heat rate of the engine.

From a maintenance and operational standpoint, engine wash is a standard procedure to both prevent the engine from permanent damage and aid in performance recovery [3]. Correct scheduling of the engine wash is extremely important to ensure optimal operation and maintenance of the engine [4], and this is only possible if the degradation behavior of the engine can be accurately tracked over time. It is also important to establish the effectiveness of each wash and its corresponding performance recovery during the operational period.

The main objective of this paper is to extend the methodology of degradation analysis, which was previously applied to a single-spool GE LM2500+ engine [5], to twin-spool RR RB211-24G and GE LM1600 engines in order to quantify the degree of engine-air-compressor degradation. The engine-air-compressor degradation is tracked through changes in the isentropic efficiency of the air compressor of the respective engine. Five engines employed at five different compressor station sites on TransCanada Pipeline system in Canada were assessed. The operational data on which the analysis is performed was acquired for operating hours spanned as far back as 2007-2009 through to August 2015.

2. Degradation Prediction Model

Gas Path Analysis (GPA) and an Error-in-Variables Model (EVM) were used to track the engine degradation over time in a manner similar to that described by Botros et al. [5]. These methods will be described in the following two subsections.

i) Gas Path Analysis

GPA refers to fundamental thermodynamic calculations to evaluate the properties (such as pressures, temperatures, fuel flow rate, etc.) of the air and the products of combustion as they pass through the various components of the engine [6]. For the GPA, three types of parameters are defined, namely:

1. Engine Parameters (y), such as pressure, temperature, fuel flow rate, shaft power etc. However, what is read by the sensors at the plant are the Measured Engine Parameters (m), which are the true engine parameters (y) distorted with noise (ε) due to instrumentation inaccuracies. ($m = y + \varepsilon$)

2. External Input Parameters (u), such as properties of the gas path, Lower Heating Value (LHV) of the fuel, spool speeds, mechanical efficiencies of the components, etc.

3. Health Parameters (*H*), which are the indicators that define the health condition of the engine, and hence the degree of degradation of its components. The air compressor health parameters are the isentropic efficiency and inlet air mass flow rate, while the engine health parameters are the heat rate and the specific work. These health parameters are calculated from the measured parameters (*m*) for a given set of input parameters (*u*). In order to track the health parameters as the inlet conditions vary, the parameters must be corrected to standard inlet conditions. The formulae for the corrected shaft speed ($N_{corrected}$), mass flow ($\dot{m}_{corrected}$), shaft power ($Sh.P_{corrected}$) and specific work ($Sp.W_{corrected}$) are given below as [7]:

$$N_{corrected} = \frac{N}{\sqrt{\theta}} \tag{1}$$

$$\dot{m}_{corrected} = \frac{\dot{m}\sqrt{\theta}}{\delta} \tag{2}$$

where θ and δ are the dimensionless ambient temperature and pressure and have values of $\theta=T_2/288.15$ and $\delta=P_2/101.325$.

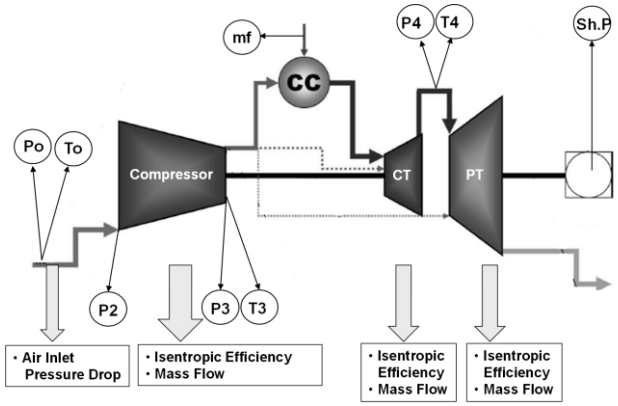

Figure 1: Schematic representation of a GT engine, with engine parameters and health parameters identified.

It is recognized that the noise in the measured parameters will propagate to the calculated health parameters, resulting in a noisy scatter (smearing) of the health parameter values. A summary of the Engine Parameters (*y*) and the Health Parameters (*H*) is schematically depicted in Figure 1, where mf and *Sh.P* represent the fuel flow rate and the shaft power respectively. The other symbols have their usual meanings.

The Gas Path Analysis was performed using the commercial software GasTurb11 [8,9]. The ambient temperature, pressure, measured compressor exit pressure and temperature, temperature at the combustor exit and the spool speed are specified as inputs. Although the RB211-24G and GE LM1600 are twin-spool engines, there is aerodynamic coupling between the shaft speeds of the two shafts [10] and therefore the health parameters for this engine are calculated assuming a single-spool arrangement. Mechanical efficiencies of the components are also fed in as fixed external input parameters along with LHV of the fuel. The procedure

completes the thermodynamic cycle of the engine operation and calculates the health parameters. However, these health parameters, as calculated by GasTurb11, are also contaminated with noise that has propagated from the measured parameters. Therefore, additional steps must be taken before data analysis is possible.

ii) Parameter Estimation – Bayesian Error-in-Variables Model (EVM)

EVM is commonly used in data modeling for obtaining point estimates of unknown parameters where all the involved variables have inherent uncertainty in them [11]. EVM finds direct relevance to the problem in hand in which all the measured variables and the health parameters from the GPA model are subject to varying degrees of inaccuracies. Ordinary Least Squares method would not be suitable for the present problem as it only corrects the dependent variable assuming the other variables to be error free [12]. Also, unlike in Ordinary Least Squares, EVM models are dependent on prior knowledge of the error structure in each and the vector of coefficient parameters used in the objective functions as of the variables involved [11] allowing more accurate estimates. Detailed discussions on EVM can be found in Keeler and Reilly [11] and Seber and Wild [13].

The EVM analysis involves defining the vector of variables involved, which must be conditioned off the noise, as:

$$\bar{Y} = \begin{pmatrix} P_2 \\ P_3 \\ T_2 \\ T_3 \\ N_{1,corrected} \\ \eta_{is} \end{pmatrix} \tag{3}$$

where P_2 and P_3 are the compressor suction and discharge pressure, T_2 and T_3 are the compressor suction and discharge temperature, $N_{1,corrected}$ is the corrected compressor shaft speed and η_{is} is the compressor isentropic efficiency. Similarly vector Y_{true} contains the true values of the variables in Y in the same order. Next, a vector of objective functions is defined as:

$$F_1 = \eta_{is} - [c_0 + c_1\Psi + c_2\Psi^2] = 0 \tag{4}$$

$$F_2 = \eta_{is} - \frac{T_2\left[\left({}^{P_3}/_{P_2}\right)^{\frac{k-1}{k}} - 1\right]}{T_3 - T_2} = 0 \tag{5}$$

where Ψ is the compressor head coefficient [10] and is defined as:

$$\Psi = \frac{H}{N_{1,corrected}^2}\Psi = \frac{1}{N_{1,corrected}^2}\frac{ZRT_2}{(k-1)/k}\left[\left(\frac{P_3}{P_2}\right)^{\frac{k-1}{k}} - 1\right] \tag{6}$$

where H, Z, R and k are the air-compressor enthalpy rise, average compressibility factor, gas constant and isentropic exponent, respectively. The vector of the coefficient parameters used in the objective function is:

$$\overline{\Theta} = \begin{pmatrix} c_0 \\ c_1 \\ c_2 \end{pmatrix} \tag{7}$$

In addition to these three coefficients, the model also requires defining the error covariance matrix ($\bar{V}$). In the error covariance matrix, the diagonal elements are the average uncertainty of each variable involved while the non-diagonal elements are the error of one variable with respect to the uncertainty in the others. For the present functions model, the covariance matrix is selected on the basis of the expected uncertainty associated with the measurement of the individual variables, implying that the errors are uncorrelated (i.e., "zeros" in the non-diagonal elements) [14]. Thus:

$$\bar{V} = \begin{pmatrix} \sigma_{P_2}^2 & 0 & 0 & 0 & 0 & 0 \\ 0 & \sigma_{P_3}^2 & 0 & 0 & 0 & 0 \\ 0 & 0 & \sigma_{T_2}^2 & 0 & 0 & 0 \\ 0 & 0 & 0 & \sigma_{T_3}^2 & 0 & 0 \\ 0 & 0 & 0 & 0 & \sigma_{N_1}^2 & 0 \\ 0 & 0 & 0 & 0 & 0 & \sigma_{\eta_{is}}^2 \end{pmatrix} \tag{8}$$

Given the range of values for the variables in question as well as the instrumentation used, the average standard deviations were chosen to be:

$$\sigma_{P_2} = 1kPa$$
$$\sigma_{P_3} = 20kPa$$
$$\sigma_{T_2} = 0.5℃$$
$$\sigma_{T_3} = 5℃$$
$$\sigma_{N_1} = 10RPM$$
$$\sigma_{\eta_{is}} = 0.05$$

The procedure in the EVM is aimed at determining the coefficients in the polynomial of Eq. 4, as well as the vector Y_{true}. This involves inner and outer iterations, the details of which are given by Botros et al. [5].

3. Results of RR RB211-24G Gas Turbine at Station #1

Table 1 shows the timeline of operation for which engine performance data were collected on the RR RB211-24G engine employed at a compressor station in Alberta, referred to as Station #1. This station is located in Alberta in the midst of forest close to the Rocky Mountains in Central Alberta, at elevation = 946 m above sea level. The site power rating of the engine at this elevation is 24.698 MW at 15 ºC.

Data acquisition began on March 1, 2010. This engine was then replaced with a new engine on August 18, 2011 after 7,766 operating hours (OH). An offline wash was performed on the new engine on June 14, 2012. The Intermediate Pressure (IP) stator was replaced on April 23, 2013, and another offline wash was performed on August 19, 2013. Another new engine replacement took place on August 13, 2014 followed by an offline

wash on June 16, 2015 and data continued to be collected until August 18, 2015 (end of data acquisition). To track the effect the engine IP stator and GG replacements, as well as the offline washes, the timeline has been separated into seven distinct periods as shown in Table 1. The OH in each period is also indicated spanning the aforementioned dates of respective events.

Table 1: Timeline of data acquisition for the RR RB211-24G engine at compressor station #1.

Date	Event	Event #
March 1, 2010	Start of Data Acquisition	
Period 1 (OH = 7766)		
August 18, 2011	New Engine Replacement	**E1**
Period 2 (OH = 4984)		
June 14, 2012	Offline Soak Wash	**E2**
Period 3 (OH = 7161)		
April 23, 2013	New IP Stator Replacement	**E3**
Period 4 (OH = 2188)		
August 19, 2013	Offline Soak Wash	**E4**
Period 5 (OH = 8158)		
August 13, 2014	New Engine Replacement	**E5**
Period 6 (OH = 6994)		
June 16, 2015	Offline Soak Wash	**E6**
Period 7 (OH = 1475)		
August 18, 2015	End of Data Acquisition	

The engine degradation and recovery (or un-recovery) is assessed based on evaluation of one of the engine health parameters shown in Fig. 1, namely, the isentropic efficiency of the air compressor. This was found to be most prone to engine degradation among other health parameters [15-17]. The approach used is that the air compressor isentropic efficiency during the last 500 OH of one period is mapped as a function of compressor pressure ratio ($P_r=P_3/P_2$) and corrected low pressure compressor spool speed ($N_{1,corrected}$), and compared to the first 500 OH of the subsequent period. It should be noted that the corrected spool speed ($N_{1,corrected}$) is that of the low pressure compressor in the case of twin spool engines. The power turbine speed is not considered here since the health parameter under consideration in the present paper is chosen to be the isentropic efficiency of the air compression section of the gas generator through the axial compressor (single spool or twin spool). Contour maps of $N_{1,corrected}$ vs. P_r colour-coded by engine-air-compressor isentropic efficiency are used to track the compressor degradation between data sets. These comparisons across each event (hardware replacements or engine washes) are shown chronologically in Fig. 2.

It is evident that the engine replacement on August 18, 2011 and August 13, 2014 significantly improved the isentropic efficiency (contrast the last 500 hrs and first 500 hrs in Figs. 2a and 2e). Figure 2c shows the effects

of the IP stator replacement indicating only slight improvement in the isentropic efficiency. Figures 2b, 2d and 2f show the effects of the three soak washes of the engine, respectively, where it can be observed that these washes have little effect on improving the isentropic efficiency. A trend noticed in all of the contour maps is the very narrow relationship observed between P_r and $N_{1,corrected}$. From the typical compressor characteristic map shown in Figure 3 [18], it can be discerned that along the maximum efficiency line there is only one $N_{1,corrected}$ for a given P_r. Therefore, the tight relationship between P_r and $N_{1,corrected}$ for this engine air compressor implies that the engine is being run very close to its maximum efficiency.

To quantitatively determine the degradation during periods as well as the improvement (or lack of) between periods, the isentropic efficiency is tracked over time for constant $N_{1,corrected}$ and P_r. Figure 4 shows the time-history of engine air compressor isentropic efficiency for three selected $N_{1,corrected}$ of 6426, 6351 and 6276 RPM, where the following general trends can be observed. The following observations can be made:

- In period 1, the compressor isentropic efficiency degrades from the beginning of the data acquisition until the engine replacement, after which the isentropic efficiency improves by approximately 1.2 percentage points.
- In period 2, the isentropic efficiency begins to degrade immediately, and continues to degrade at a constant rate through to the end of period 3, decreasing by 2.5 percentage points in the 12,145 total OH of periods 2 and 3 combined. Note that the first offline wash only slightly improves the isentropic efficiency, with an increase of 0.3 percentage points.
- The IP replacement between periods 3 and 4 improves the isentropic efficiency by approximately 0.5 percentage points.
- Periods 4 and 5 (combined) show a decrease in the isentropic efficiency by approximately 1.0 percentage point over a relatively long OH of 10346 hours. Again the second offline wash of the engine did not result in significant improvement in the isentropic efficiency.
- The new engine replacement on August 13, 2014 resulted in a significant recovery of compressor isentropic efficiency of approximately 0.33 percentage points, while the last offline wash on June 16, 2015 again did not seem to recover the degradation that occurred during period 6. Note that the above-mentioned trends are consistent across all three $N_{1,corrected}$.

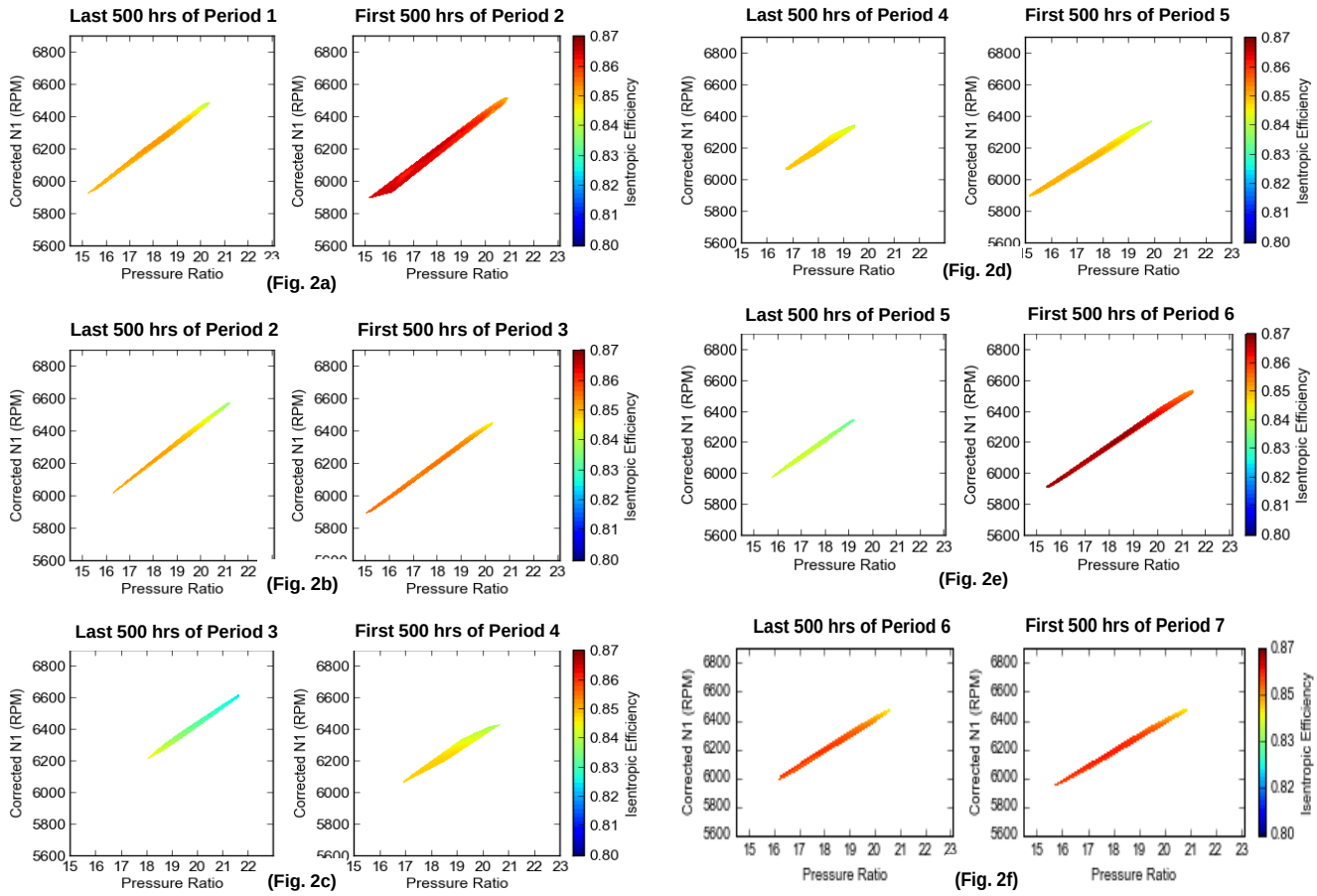

Figure 2: Contour map of engine air compressor isentropic efficiency changes before and after each event of the RB211-24G engine employed at Station #1.

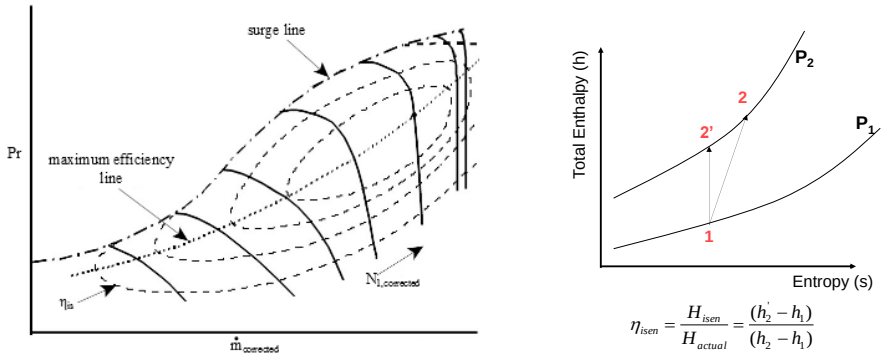

Figure 3: Typical axial compressor characteristic map [18].

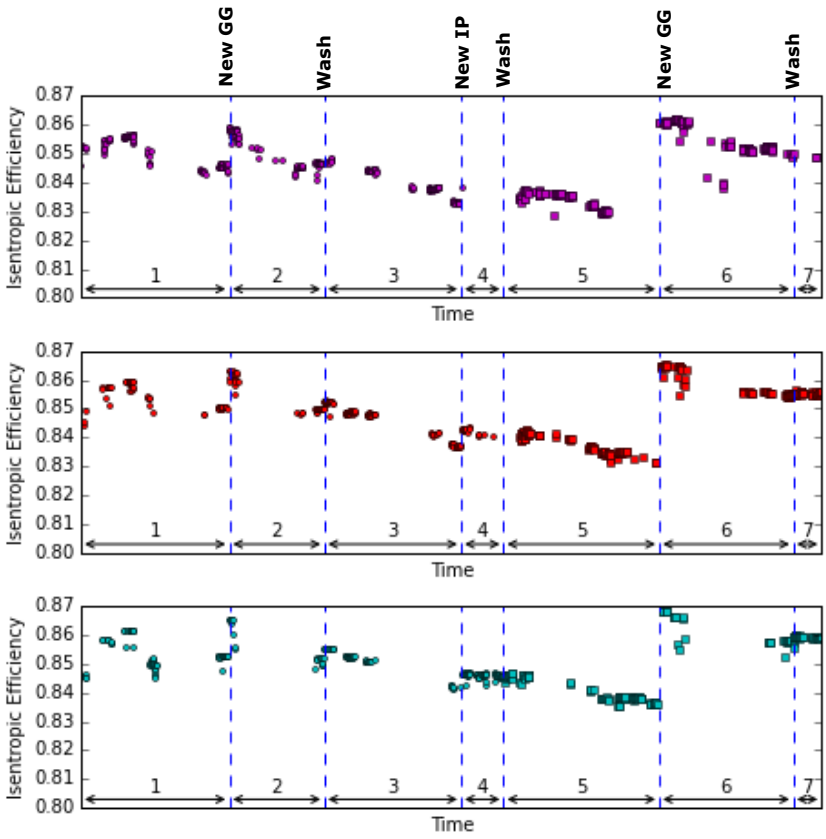

Figure 4: Engine-air-compressor isentropic efficiency of RB211-24G at Station #1 vs. time for $N_{1,corrected}$ = 6426, 6351 and 6276 RPM, from top to bottom.

4. Results of GE LM2500+ at Station #2

The second gas turbine engine is a GE LM2500+ employed at compressor station site #2. This station is located in the Saskatchewan prairies surrounded by farm land, and at elevation = 730 m above sea level. The site power rating of the engine at this elevation is 27 MW at 15 ^{o}C.

This engine was installed after a hot section repair on April 8, 2009 and has been running since then. Data were collected since this date up to August 18, 2015. Six offline washes have been performed during this time. Table 2 shows the timeline of these washes and identification of seven periods and respective OH. Similar to the analysis of the RB211-24G engine, the degradation of the LM2500+ engine air compressor is examined for each period to determine the degree of recoverable vs. un-recoverable degradation. Again, the indicator is the air compressor isentropic efficiency as the most susceptible engine health parameter prone to engine degradation.

Table 2: Timeline of data acquisition for the GE LM2500+ engine at compressor station #2.

Date	Event	Event #
April 8, 2009	New Engine Installed	
Period 1 (OH = 3310)		
November 6, 2009	Offline Soak Wash	**E1**
Period 2 (OH = 3176)		
April 27, 2010	Offline Soak Wash	**E2**
Period 3 (OH = 3800)		
March 24, 2011	Offline Soak Wash	**E3**
Period 4 (OH = 3841)		
May 26, 2012	Offline Soak Wash	**E4**
Period 5 (OH = 3014)		
December 2, 2013	Offline Soak Wash	**E5**
Period 6 (OH = 4954)		
April 14, 2015	Offline Soak Wash	**E6**
Period 7 (OH = 426)		
August 18, 2015	End of Data Acquisition	

Figure 5 shows contrasting contour maps of the air compressor isentropic efficiency of the last 500 OH of one period compared to the first 500 OH of the subsequent period (except for period 7 which had only 426 OH until August 18, 2015). Again, the contour maps are presented in terms of $N_{1,corrected}$ vs. P_r color-coded by engine air compressor isentropic efficiency. Unlike the previous station, this LM2500+ engine has been operating without any hardware replacement since its hot section repair in April 2009, and hence is a good example of an engine to demonstrate the effectiveness of periodical soak washes. It is clear from contrasting the color-coded maps in Fig. 5 that the engine significantly benefited from the offline washes in the evaluated period of time. The only exception is the first engine wash between period 1 and period 2. In fact, it was found that during period 1, almost no degradation was observed during this period, and under some conditions there was a slight improvement in the performance of the engine between the first and middle 500 hours of operation. The engine seemed to be in fairly good condition when the first soak wash was performed, which suggested that this specific wash may not have been necessary. All other subsequent engine washes resulted in quite an improvement in the engine air compressor isentropic efficiency, particularly between periods 3 and 4, and periods 6 and 7. This overall improvement after engine washes (with the exception of the first) is in contrast to the case of the RB211-24G engine, where a small increase in isentropic efficiency was observed after the first offline wash. Also in contrast to the RB211-24G engine is the observation that there is much more wider operating range in terms of $N_{1,corrected}$ vs. P_r (compare Fig. 2 to Fig. 5). Referring back to Figure 3,

this wider range implies that the LM2500+ engine air compressor is not operating at the maximum isentropic efficiency. Additionally, since this engine is operating in the midst of a farm land in the Saskatchewan prairies, the air quality is prone to be not as pure as that in the mountain forest (i.e. Station #1). Hence, engine washes seem to be effective in Station #2 than in Station #1.

Similarly, to quantitatively determine the degradation during periods as well as the improvement following each wash, the isentropic efficiency is tracked over time for constant $N_{1,corrected}$ and P_r. Figure 6 shows the time-history of compressor isentropic efficiency for $N_{1,corrected}$ of 9669, 9594 and 9519 RPM, where the following general trends can be observed:

- Between periods 1 and 2, there is hardly any improvement, but between periods 2 and 3 there is a gain of 1.2 percentage points after the engine wash.
- Between periods 3 and 4, after the third offline wash, the isentropic efficiency increases by 2.2 percentage points.
- During period 4, the efficiency degrades by 1 percentage point, and subsequently recovers 1 percentage point before the fourth offline wash. Similar trend is observed in period 5.
- As for the offline wash between periods 5 and 6, it appears that the engine lost one percentage point of isentropic efficiency as is also demonstrated in the contour maps in Fig. 5e.
- The last soak wash after period 6 shows a recovery of 1.1 percentage point in isentropic efficiency. Note that all of the above mentioned trends are consistent across all three $N_{1,corrected}$.

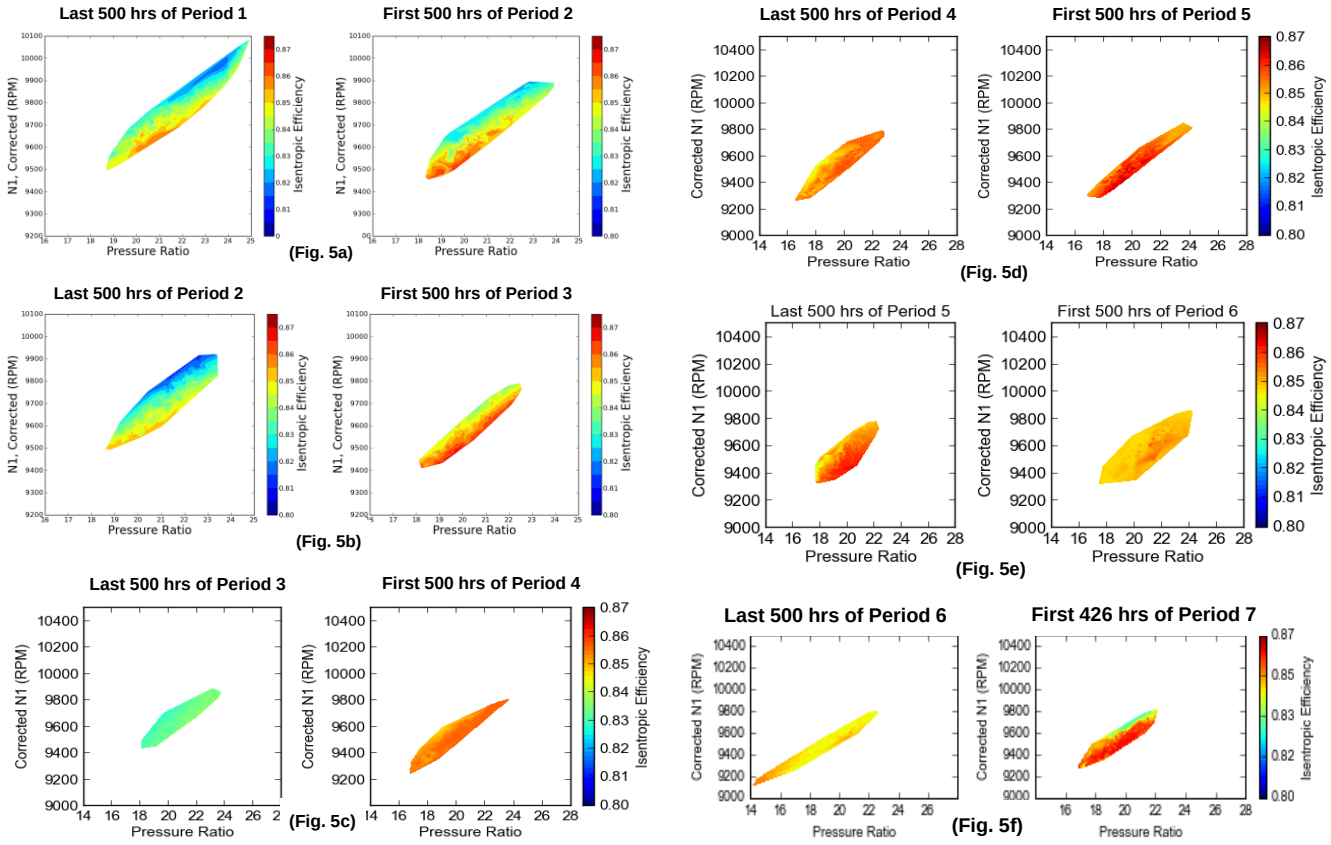

Figure 5: Contour map of engine air compressor isentropic efficiency changes before and after each event of the LM2500+ engine employed at Station #2.

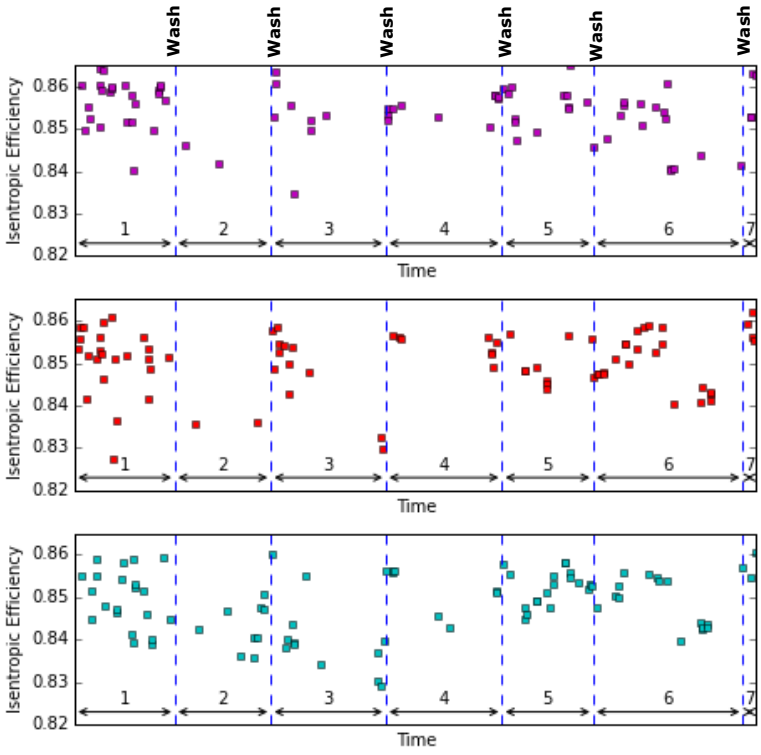

Figure 6: Engine-air-compressor isentropic efficiency of LM2500+ at Station #2 vs. time for $N_{1,corrected}$= 9669, 9594 and 9519 RPM, from top to bottom.

5. Results of GE LM2500+ at Station #3

The third gas turbine engine is also a GE LM2500+ employed at compressor station site #3. This station is located in the forested area in Ontario, and at elevation = 741 m above sea level. The site power rating of the engine at this elevation is 27.25 MW at 15 ^{o}C.

Data were collected from January 1, 2008 through to August 18, 2015. The total number of OH during this almost 7 years is 16,883 hours. Two offline washes have been performed during this time. Table 3 shows the timeline of these washes and identification of three periods and respective breakdown of the OH. Similar to the analysis of the previous two engines, the degradation of the engine air compressor is examined for each period to determine the degree of degradation levels during each of the three periods.

Figure 7 shows contrasting contour maps of the air compressor isentropic efficiency of the last 500 OH of one period compared to the first 500 OH of the subsequent period. It is shown that period 1 has the longest OH that the engine has been operating without a wash. As a result, there is 1.0-1.5 percentage points decrease in the air-compressor isentropic efficiency during this period. The second wash that followed after 4,110 OH in the period 2 did not seem to have benefited the engine as is seen from contrasting the color-coded maps in Fig. 7b.

Figure 8 shows the time-history of compressor isentropic efficiency for $N_{1,corrected}$ of 9115, 9315, 9515, 9715 and 9915 RPM. The data in this Figure substantiate the previous observation on Fig. 7 in that the second engine wash did not seem to benefit the engine, while the first did. It is also shown that there is appear to be an improvement in the middle of period 1. The reason for this improvement is not known. It is suspected that there could have been a hardware replacement on the engine without accurately logging the upgrade in the engine log-book. This was also observed (to a lesser extent) of the pattern in period 5 on Fig. 6 for Station #2.

Table 3: Timeline of data acquisition for the GE LM2500+ engine at compressor station #3.

Date	Event	Event #
January 1, 2008	Start of Data Acquisition	
Period 1 (OH = 7169)		
February 3, 2009	Offline Soak Wash	**E1**
Period 2 (OH = 4110)		
August 20, 2012	Offline Soak Wash	**E2**
Period 3 (OH = 5604)		
August 18, 2015	End of Data Acquisition	

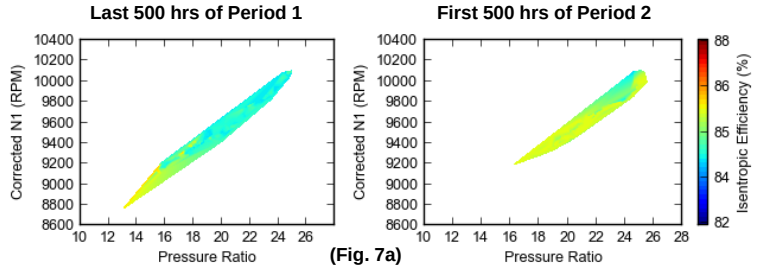

(Fig. 7a)

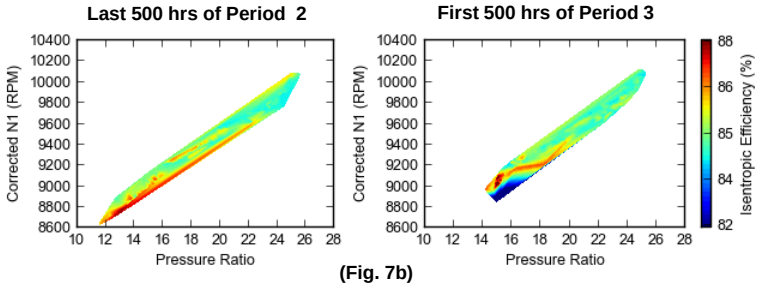

(Fig. 7b)

Figure 7: Contour map of engine air compressor isentropic efficiency changes before and after each event of the LM2500+ engine employed at Station #3.

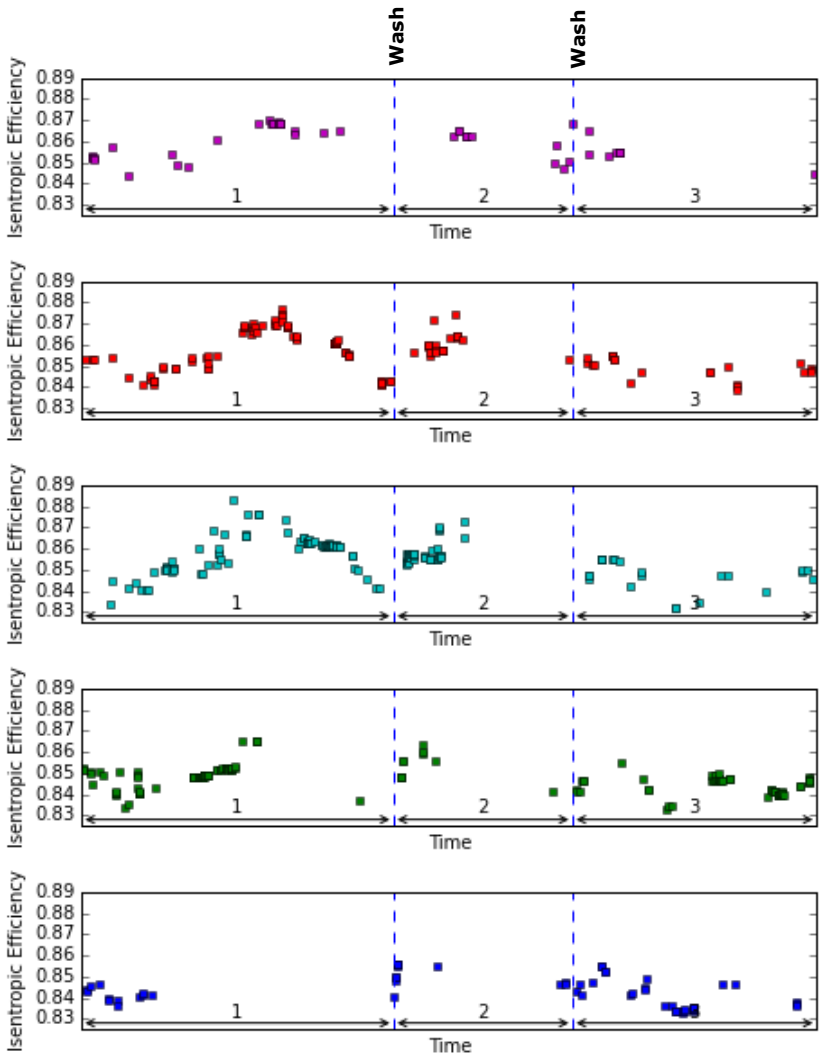

Figure 8: Engine-air-compressor isentropic efficiency of LM2500+ at Station #3 vs. time for $N_{1,corrected}$ = 9115, 9315, 9515, 9715 and 9915 RPM, from top to bottom.

6. Results of GE LM2500+ at Station #4

The fourth gas turbine engine is also a GE LM2500+ employed at compressor station site #4. This station is located in a forested area in southern Alberta, and at the highest elevation of all of the five engines examined in this paper (elev. = 1,359 m above sea level). The site power rating of the engine at this elevation is 24.881 MW at 15 ºC.

Data were collected from December 23, 2013 through to August 18, 2015. Two washes were conducted on this engine since the time of the start of the data acquisition. Table 4 shows the timeline of these two washes and identification of three periods and the respective breakdown of the OH.

Figure 9 shows contrasting contour maps of the air compressor isentropic efficiency of the last 500 OH of one period compared to the first 500 OH of the subsequent period. It is shown that the first engine wash on May 8, 2014 has resulted in slight improvement in the compressor isentropic efficiency of the order of approximately 0.45 percentage point. Slightly smaller improvement (approx. 0.375 percentage point) is noted after the second wash on October 16, 2014.

Figure 10 shows the time-history of compressor isentropic efficiency for $N_{1,corrected}$ of 9180, 9330, 9480, 9630 and 9780 RPM. These data also show the approximate gain in the compressor isentropic efficiency of approximately 0.4 percentage point after each of the two engine washes reported during this evaluation period. The condition of the engine after the third offline wash on July 13, 2015 could not be determined since the OH after this wash was only 71 hours till the end of data acquisition on August 18, 2015. This will be evaluated in the future once the engine has run for at least 500 hours post this last wash.

Table 4: Timeline of data acquisition for the GE LM2500+ engine at compressor station #4.

Date	Event	Event #
December 23, 2013	Start of Data Acquisition	
Period 1 (OH = 2230)		
May 8, 2014	Offline Soak Wash	E1
Period 2 (OH = 1895)		
October 16, 2014	Offline Soak Wash	E2
Period 3 (OH =3323)		
July 13, 2015	Offline Soak Wash	E3
Period 4 (OH = 71)		
August 18, 2015	End of Data Acquisition	

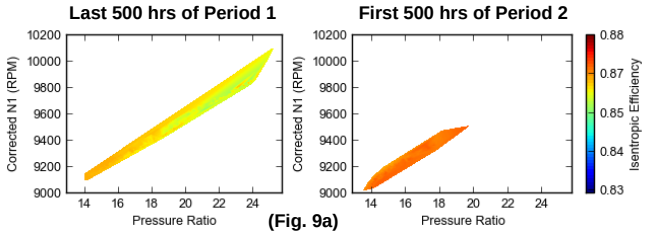

Figure 9: Contour map of engine air compressor isentropic efficiency changes before and after each event of the LM2500+ engine employed at Station #4.

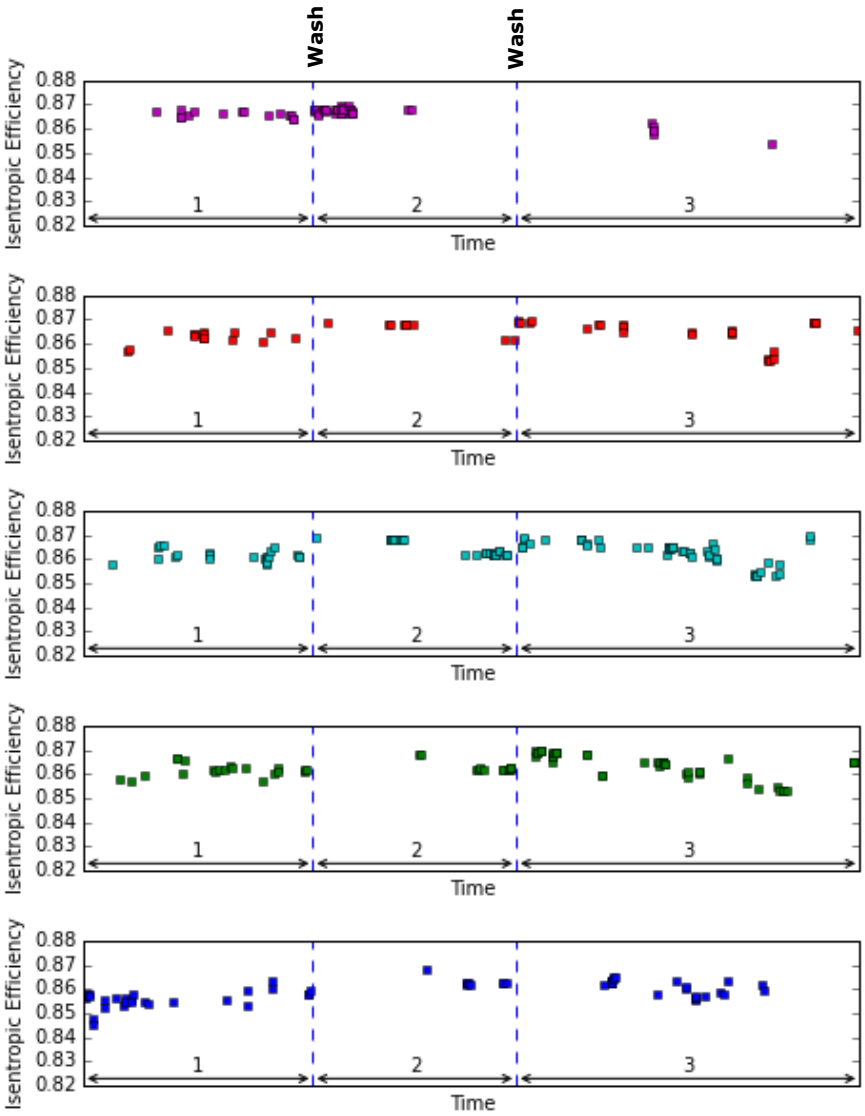

Figure 10: Engine-air-compressor isentropic efficiency of LM2500+ at Station #4 vs. time for $N_{1,corrected}$ = 9180, 9330, 9480, 9630 and 9780 RPM, from top to bottom.

7. Results of GE LM1600+ at Station #5

The last gas turbine engine is a GE LM1600 employed at compressor station site #5. This station is located in the forested area in southern British Columbia (Canada), and at elevation = 843 m above sea level. The site power rating of the engine at this elevation is 12.709 MW at 15 ^{o}C.

Data were collected from December 14, 2007 through to August 18, 2015. Four offline washes have been performed during this time. Table 5 shows the timeline of these washes and identification of five periods and respective breakdown of the OH. Similar to the analysis of the previous four engines, the degradation of the engine air compressor is examined for each period to determine the degree of degradation during each of the four periods.

Figure 11 shows the contrasting contour maps of the air compressor isentropic efficiency of the last 500 OH of one period compared to the first 500 OH of the subsequent period. The color coded isentropic efficiency in all of these maps are very close, indicating that the engine is generally running cleanly without noticeable degradation whatsoever. This could be due to the air quality in the area of the compressor station site and also the total number of OH over this relatively long time (approximately 8 years).

Figure 12 shows the corresponding time-history of compressor isentropic efficiency for $N_{1,corrected}$ of 12530, 12630, 12730, 12830 and 12930 RPM. The data in this Figure substantiate the previous observation in that the three engine washes did not seem to benefit the engine. This again could be attributed to air quality and likely due to the generally low part load this engine was running at as will be discussed in the next Section. There is, however, a noticeable increase in the isentropic efficiency of approximately 0.74 percentage point in the following January 30, 2015 engine service, which include some compressor work and components replacement.

Table 5: Timeline of data acquisition for the GE LM1600 engine at compressor station #5.

Date	Event	Event #
December 14, 2007	Start of Data Acquisition	
Period 1 (OH = 2303)		
Septemebr 20, 2008	Offline Soak Wash	**E1**
Period 2 (OH = 2231)		
November 16, 2009	Offline Soak Wash	**E2**
Period 3 (OH = 4048)		
September 23, 2013	Offline Soak Wash	**E3**
Period 4 (OH = 2552)		
January 30, 2015	Components Relpacement	**E4**
Period 5 (OH = 1599)		
August 18, 2015	End of Data Acquisition	

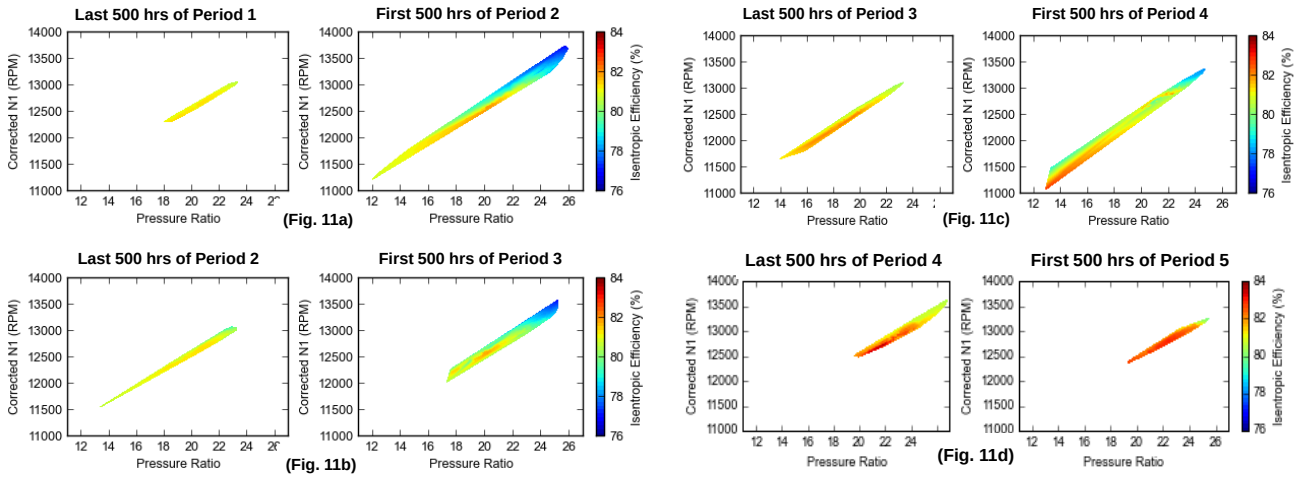

Figure 11: Contour map of engine air compressor isentropic efficiency changes before and after each event of the LM1600 engine employed at Station #5.

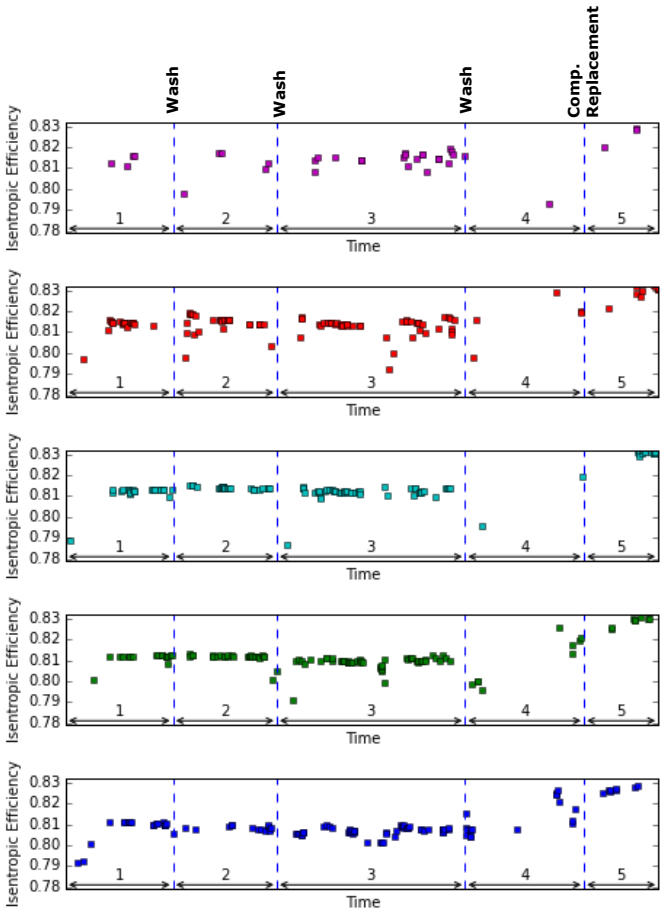

Figure 12: Engine-air-compressor isentropic efficiency of LM1600 at Station #5 vs. time for $N_{1,corrected}$=12530, 12630, 12730, 12830 and 12930 RPM, from top to bottom.

8. Discussion

From all of the foregoing data of gas turbine engine degradation over varying OH of periods between soak washes or hardware replacement, it could be possible to distinguish degradations that were recovered following an engine wash, and those that were attributed to normal wear of the engines due to the predominantly the overall OH.

The recoverable degradation is easy to discern, which is manifested by the step gain in the isentropic efficiency (η_{is}) of the air compressor following each engine wash. Table 6 shows a summary of these isentropic efficiency gains after each event (offline wash or hardware replacement) for each of the five engines examined. The gain in η_{is} is averaged over the first 500 OH after the event vs. the last 500 OH before the event. The standard deviation in the average η_{is} was 0.05 percentage point. The total engine air intake flow during the period prior to the event is also recorded in the Table and normalized by engine rated site power to allow valid comparison given that the fifth engine is rated at a much lower power than the first four. For each engine, a general trend can be observed, in that the gain in η_{is} after each wash correlates with the amount of air intake during the period preceding the event. This is a reasonable metric, since more air mass breathed by a given engine the more it will be prone to accumulate dusts, and hence a soak wash will be more effective to recover the resulting degradation. It should be noted that this is valid when events are compared among themselves for the same engine and not across all engines, since they are employed at different sites with different air quality. It should be noted that an recoverable isentropic efficiency on the order of 1.0 percentage point constitute an economically significant gain in engine performance which amounts to approximately 0.52 MW reduction in the air compressor power of an engine based on 24 MW shaft power. This translates to 150 GJ per day saving in fuel.

Table 6: Comparison of the recoverable degradation of the five engines evaluated in the present work.

Event	OH from Previous Period	Gain in η_{is}	Air Intake during the period prior to the event	Average Site Rated Power	Air Intake / Average Site Rated Power
		(% points)	(10^6 kg)	(MW)	(10^6 kg/MW)
Station #1					
E1*	7766	1.2	1949	25.8	75.6
E2	4984	0.3	1304	26.8	48.6
E3	7161	0.5	1816	26.7	68.0
E4	2188	0.1	515	24.4	21.1
E5*	8158	3.3	2023	26.4	76.5
E6	6994	0.07	1797	26.5	67.8
Station #2					
E1	3310	?	856	27.9	30.7
E2	3176	1.2	868	30.4	28.6
E3	3800	2.2	1025	30.0	34.2
E4	3841	0.2	969	29.4	33.0
E5	3014	0.5	706	28.2	25.1
E6	4954	1.1	1126	29.3	38.4
Station #3					
E1	7169	1.3	1744	30.1	57.9
E2	4110	0.2	1003	30.5	32.9
Station #4					
E1	2230	0.45	312	27.9	11.2
E2	1895	0.375	251	25.3	9.9
Station #5					
E1	2303	0	308	12.9	23.9
E2	2231	0	320	12.5	25.6
E3	4048	0	564	12.4	45.5
E4*	2552	0.3	374	13.8	27.1

* Engine replacement

The un-recoverable degradation can also be determined from the data analysis presented earlier for each engine. An un-recoverable degradation in terms of the loss in the air compressor isentropic efficiency over a period can be determined from the difference in isentropic efficiency immediately after each successive event. If the difference is negative, it is indicative of un-recoverable degradation, and if the difference is positive it is indicative of a gain likely due to an engine repair or hardware replacement. Table 7 shows the results of these

un-recoverable degradations during the various periods between events for the five engines evaluated in terms of loss of isentropic efficiency per 1000 OH. It is shown that, for the most part, the unrecoverable degradation (per 1000 OH) becomes more pronounced as the engine loading increases. The strange positive un-recoverable degradation shown for period 4 of for Station #2 is attributed to the previous offline wash being not effective.

The rate of recoverable and unrecoverable degradation for the five engines is found to be correlated to the engine location and operating mode (% load and operating range). As indicated earlier, station #2 is located in the prairie with potential for air-borne dust to be breathed into the Engine. This is in contrast to the other stations located in the forest with much cleaner air. Hence recoverable degradation appears to be more pronounced for the engine in Station #2 than the rest. On the other hand, the RB211-24G is constantly running near capacity (i.e., base-loaded), the engine parts are likely to wear out. The un-recoverable degradation of this engine seems to be the highest, and hence it was subject to an IP stator replacement and a GG change out in three years (see Table 1).

An alternate explanation for the type of degradation that each engine experiences is based on the operating hours between offline washes. For the RB211-24G engine, there are more operating hours between engine washes. If there is air-borne dust breathed into the engine air compressor, operating the engine for too long between offline washes may result in prolonged contact between the dust and engine parts, thus resulting in the wearing down of engine parts (unrecoverable degradation). However, if there are less operating hours between offline washes, as is the case for the LM2500+ and LM1600 engines, then air-borne dust will be washed before it has a chance to wear down the engine parts, thus avoiding unrecoverable degradation.

Table 7: Comparison of the un-recoverable degradation of the five engines evaluated in the present work.

	Un-recoverable Deg. (Loss in η_{is})	Average Shaft Load During the Period	Site Rated Power	Average Shaft Power / Rated Power
Period	(% points / 1000 OH)	(MW)	(MW)	-
Station #1				
2	-0.19	21.697	26.815	0.81
3	-0.13	21.157	26.715	0.79
4	-0.05	18.275	24.437	0.75
6	-0.14	21.4	26.5	0.81
Station #2				
1	0	21.799	27.882	0.78
2	0	24.831	30.391	0.82
3	-0.08	21.959	30.005	0.73
4*	0.09	21.093	29.386	0.72
5	-0.28	20.065	28.152	0.71
6*	0.17	21.1	29.3	0.72
Station #3				
1	-	20.718	30.126	0.69
2	-0.17	20.174	30.483	0.66
Station #4				
1	0.72	13.938	27.946	0.50
2	0.03	12.186	25.265	0.48
Station #5				
1	-	8.716	12.863	0.68
2	-0.18	9.595	12.509	0.77
3	-0.09	9.263	12.388	0.75
4**	0.74	10.1	13.8	0.73

* Previous wash was ineffective

** Engine service on January 30, 2015

9. Conclusions

The following five main conclusions can be drawn from the present investigation:

1. For a given gas turbine engine, recoverable degradation (recoverable by means of soak wash) correlates well with cumulative engine air intake between soak washes for that engine at the specific site condition.

2. The rate of un-recoverable degradation in terms of permanent loss in compressor isentropic efficiency per 1000 OH correlates well with engine loading (defined as hourly averaged shaft power / site rated power).

3. The RB211-24G engine installed at Station 1 is base-loaded and operated on a tight range along the maximum compressor efficiency line, while the LM2500+ and LM1600 engines installed at other Stations are operated over relatively wider ranges at part loads. As such, RB211-24G engine seems to be subjected to un-recoverable degradation more than the rest and needed to be overhauled after three years.

4. Engines employed in compressor stations in a forested area degraded (from recoverable sense) at a much lower rate than engines located in the prairies. Hence, frequency of engine washes is not critical for the former as compared to the latter.

5. An extension of the current work (i.e. future work) could include assessment of the air filtration performance on each engine, and their impact on respective engine degradation (recoverable vs. un-recoverable), particularly since the five engines examined in the present work are located at different sites of different air quality and environment.

10. Acknowledgments

The authors wish to acknowledge the discussion and technical dialogue with Ken Meszaros, Landen Stein and Curtis Phinney on the operation of the five engines discussed in this paper. The support of TCPL Technology Management; Thomas Robinson, Anthony Tse and Tracy Cairns during the course of this work is greatly appreciated. This paper is part of a research program sponsored by TransCanada Pipelines Ltd., and permission to publish is gratefully acknowledged.

NOMENCLATURE

c_0-c_2	coefficients of objective function F_1
F	vector of objective functions
GG	gas generator
H	engine health parameter vector, or air-compressor enthalpy rise (equation 8)
IP	intermediate pressure
k	isentropic exponent
m	measured engine parameter vector
$\dot{m}$	engine-air-compressor air inlet flow rate (kg/s)
N_1	engine-air-compressor low shaft speed (rpm)
P_2	engine-air-compressor suction pressure (kPa)
P_3	engine-air-compressor discharge pressure (kPa)
P_r	engine-air-compressor pressure ratio

R	gas constant (kJ/mol-K)
Sh.P	shaft output power (kW)
T_2	engine-air-compressor suction temperature (K)
T_3	engine-air-compressor discharge temperature (K)
u	external input parameters
V	error covariance matrix
y	true engine parameters
Z	average compressibility factor
δ	corrected pressure
ε	random error or noise
η_{is}	engine-air-compressor isentropic efficiency
θ	corrected temperature
$\overline{\Theta}$	vector of fitting parameters
σ	standard deviation in measured parameters
Ψ	compressor head coefficient

11. References

1. R. Kurz and K. Brun, "Degradation in gas turbine systems," J Eng Gas Turb Pwr - Transactions of the ASME, vol. 123, no. 1, pp. 70-77, 2001.
2. R. Kurz, K. Brun and M. Wollie, "Degradation Effects on Industrial Gas Turbines," J Eng Gas Turb Pwr - Transactions of the ASME, vol. 131, no. 6, 2009.
3. M. Morini, M. Pinelli, P. R. Spina and M. Venturini, "Numerical Analysis of the Effects of Nonuniform Surface Roughness on Compressor Stage Performance," J Eng Gas Turb Pwr - Transactions of the ASME, vol. 133, no. 7, 2011.
4. M. Fast, M. Assadi and S. De, "Condition based maintenance of gas turbines using simulation data and artificial neural network: A demonstration of feasibility," in Proceedings of the ASME Turbo Expo 2008, Berlin, Germany, 2008.
5. K. K. Botros, H. Goldshan and D. Rogers, "Effects of Engine Wash Frequency on GT Degradation in Natural Gas Compressor Stations," in Proceedings of ASME Turbo Expo 2013, San Antonio, USA, 2013.
6. Y. Li, "Gas Turbine Performance and Health Status Estimation Using Adaptive Gas Path Analysis," J Eng Gas Turb Pwr - Transactions of the ASME, vol. 132, no. 4, 2010.
7. A. J. Volponi, "Gas Turbine Parameter Corrections," J Eng Gas Turb Pwr - Transactions of the ASME, vol. 121, pp. 613-621, 1999.
8. J. Kurzke, "Effects of inlet flow distortion on the performance of aircraft gas turbines," J Eng Gas Turb Pwr - Transactions of the ASME, vol. 130, no. 4, 2008.
9. J. Kurzke, "About simplifications in gas turbine performance calculations," in Proceedings of the ASME Turbo Expo 2007, Montreal, Canada, 2007.
10. H. I. H. Saravanamutto, G. Rogers, H. Cohen and P. V. Straznicky, Gas Turbine Theory, 6th ed., Pearson Prentice Hall, 2009.
11. S. E. Keeler and P. M. Reilly, "The error-in-variables model applied to parameter-estimation when the error covariance matrix is unknown," Can. J. Chem. Eng., vol. 69, no. 1, pp. 27-34, 1991.
12. P. M. Reilly and H. Patino-Leal, "A bayesian study of the error-in-variables model," Technometrics, vol. 23, no. 3, pp. 221-231, 1981.
13. G. A. F. Seber and C. J. Wild, Nonlinear Regression, New York: John Wiley and Sons, 1989.
14. P. Valko and S. Vajda, "An extended marquardt-type procedure for fitting error-in-variables models," Computer Chem. Eng., vol. 11, no. 1, pp. 37-43, 1987.
15. C. Hartloper, K.K. Botros, H. Golshan, D. Rogers, and Z. Samoylove: "Comparison of Degradation of two Different Gas Turbine Engines in Natural Gas Compressor Stations," Proceedings of the ASME 2014 International Pipeline Conference, IPC-2014-33015, September 29-October 3, 2014, Calgary, Alberta, Canada.

16. Botros, K.K., Hartloper, C., Golshan, H. and Rogers, D.: "Assessment of Recoverable vs. Unrecoverable Degradations of Gas Turbines Employed in Five Natural Gas Compressor Stations", Proceedings of ASME Turbo Expo 2015: Turbine Technical Conference and Exposition, Montréal, Canada, June 15 - 19, 2015.
17. Botros, K.K., Hartloper, C., Golshan, H. and Rogers, D.: "Recoverable vs. Unrecoverable Degradations of Gas Turbines Employed in Five Natural Gas Compressor Stations", ASME J. Eng. Gas Turbines Power (in press), 2015.
18. N. A. Cumpsty, Compressor Aerodynamics, John Wiley & Sones, 1989.